Applied Catalysis B: Environmental 117–118 (2012) 18–28

Contents lists available at SciVerse ScienceDirect

Applied Catalysis B: Environmental

journal homepage: www.elsevier.com/locate/apcatb

Efficient conversion of 1,2-dichlorobenzene to mucochloric acid with ozonation catalyzed by V_2O_5 loaded metal oxides

Estelle C. Chetty, Venkat B. Dasireddy, Suresh Maddila, S.B. Jonnalagadda*

School of Chemistry, University of KwaZulu-Natal, Westville campus, Chiltern Hills, Durban 4000, South Africa

ARTICLE INFO

Article history:
Received 30 September 2011
Received in revised form
10 December 2011
Accepted 3 January 2012
Available online 10 January 2012

Keywords:
Dichlorobenzene
Ozone
Vanadium pentoxide loaded
Alumina
Silica
Titania
Mucochloric acid

ABSTRACT

Ozone initiated oxidation of 1,2-dichlorobenzene (DCB) in aqueous system catalyzed by different loadings of V_2O_5 supported on metal oxides namely; Al_2O_3, SiO_2 and TiO_2 was investigated. Catalyst materials were characterized by different surface techniques including BET, TPD, SEM, FT-IR, ICP, and XRD methods. Mucochloric acid (MCA) was identified to be main oxidation product. The conversion and selectivity of MCA were compared. With 5% V_2O_5, all three supports gave 100% conversion and 100% selectivity after 5 h ozonation. Conversion efficiency of the support was $SiO_2 > Al_2O_3 > TiO_2$ for 2 h ozonation duration and 5% V_2O_5 loaded catalysts registered higher conversions than with 1% loaded. Probable reaction scheme is described.

1. Introduction

Organochlorines are harmful due to their persistence, toxicity and capacity to accumulate in the living bodies [1]. Chlorination is one of processes to inactivate the pathogenic microorganisms in aqueous environment, but it often initiates the formation of less oxidizable or more toxic by-products than the parent compounds [2]. When chlorine is used to treat waters containing naturally occurring organic matter, chlorinated by-products such as chloroform, chlorodibromomethane, bromodichloro-methane, bromoform, haloacetic acids, haloacetonitriles, haloketones and chloropicrin could form [3]. Ozone is one of the most effective oxidants, which have been widely used in water and wastewater treatment. Ozonation is preferred to chlorination, and is frequently adopted to remove the herbicides from drinking water [4]. Ozonation of halogenated organic compounds in aqueous media has been studied by many researchers and reported formation of bromate as a by-product can be minimized by ozonation at pH < 7 [5,6]. In presence of organic matter, while minimizing the formation of bromate, ozonation could incorporate bromide into organic molecules to form brominated trihalomethanes, bromodichloromethane, dibromochloromethane, bromoform, bromoacetic acids, bromoacetonitriles, etc. [7]. Ozonation has many advantages over chlorination like; it does not require additional processes to remove excess bactericidal agents from water hence higher doses of ozone can be used. A number of organic pollutants in aqueous environment such as phenols, amides, carboxylic acids, aromatics and halogenated derivatives are decomposed by ozonation by producing other oxygenated organic products, which are in more biodegradable [8].

To improve the performance of ozonation, ozone-based advanced oxidation processes (AOPs) such as O_3/UV, O_3/H_2O_2, O_3/OH, O_3/UV/TiO_2 and homogeneous or heterogeneous catalytic ozonation have been reported and employed for oxidation of several pesticides and water treatments [9]. Decomposition of trichloroethene by ozone-adsorbed silica/zeolites has been investigated due to high stability of ozone than dissolved in water. Depending on the type of catalyst and organic moiety the adsorption of diffusion of organics on the surface of the catalysts or the concentrations of $^{\bullet}$OH radicals produced on the solid/liquid interface is considered to be main responsible for the improvement of ozonation induced by the catalysts. The effectiveness of ozonation depends on the nature of catalyst, solution pH and ozone decomposition reactions. Metal oxide supported catalysts show high activity. Vanadium peroxide is widely used as heterogeneous catalyst for various controlled oxidation processes. Vanadium oxide supported catalysts are active in a wide range of applications, such as selective oxidations of several alkanes and alkenes, reduction of nitrogen oxides to ammonia. Vanadia-titania catalysts prepared by sol–gel procedures were studied as heterogeneous catalysts for the liquid

* Corresponding author. Tel.: +27 31 260 7325; fax: +27 31 260 3091.
E-mail address: jonnalagaddas@ukzn.ac.za (S.B. Jonnalagadda).

0926-3373/$ – see front matter © 2012 Elsevier B.V. All rights reserved.
doi:10.1016/j.apcatb.2012.01.004

phase oxidation of limonene and of NO_X emissions from stationary sources [10].

1,2-Dichlorobenzene (DCB) is a colorless pale yellow liquid with low water solubility and binds to soil as well in sediment. In soil, DCB is not easily broken down by soil organisms, but absorbed by aquatic plants and animals which have the ability to store and concentrate the substances in their fatty tissues) [11]. Many chlorinated organic do not have any strong nucleophilic sites, hence they are not easily prone to oxidation. Furthermore, oxidation could generate the sub products which are more toxic than the original contaminants [12]. Thus, the nature of products formed due to the ozone oxidation of DCB is to be evaluated. The present study focuses on the ozone initiated oxidation of dichlorobenzene in aqueous conditions catalyzed by vanadium pentoxide loaded on alumina, silica and titania supports.

2. Experimental

2.1. Material and method

Ozone was generated using a Fischer Ozone 500 generator, which produced ozone by the electric discharge of oxygen from a compressed oxygen cylinder via the corona discharge method. Ozone gas was bubbled into a 50 cm^3 reactor through a sintered porous diffuser with porosity 2. All experiments were carried out under ambient conditions (20 ± 1) °C at a flow rate of 1.0 L/min (LPM) and concentration of 1.094 mg/L. Fig. 1 illustrates the dimensions of the semi-batch reactor used. A magnetic stirrer was placed at the bottom of the reaction vessel to ensure maximum contact of the substrate with ozone by continuous stirring. The amount of ozone was estimated by volumetric method trapping it in KI solution and titrating the liberated iodine using standard thiosulfate solution with starch as indicator [13]. Flow rates and ozone concentrations were calibrated and high reproducible. Parameters were checked in duplicate runs, prior to and after each of the experiments. Due long durations of the experiments, each of 2 h, 4 h and 5 h experiments were repeated in duplicate. Results were highly reproducible and with less than 5% difference. Where difference was greater, such experiments replicated and data with less than 5% differences were only considered. As most of the experiments were done only in duplication, statistical analysis of the results could not be undertaken. In all cases although differences were small, trends were consistent, hence cautious approach is taken while comparing the results.

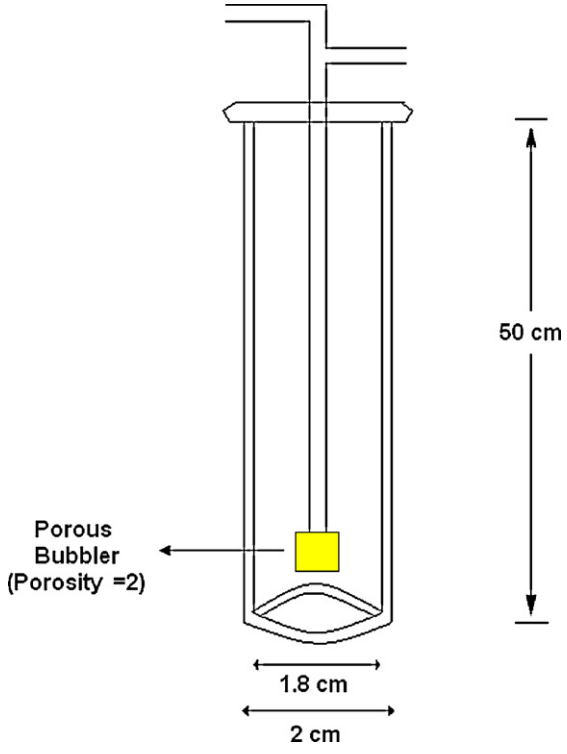

Fig. 1. Dimensions of reactor used in ozonation reactions.

The wet impregnation method was employed in the preparation of metal oxide supported catalysts. The catalysts were prepared by wet impregnation method by dissolving appropriate amount of vanadium pentoxide in distilled water (20.0 ml) and adding it to 10 g of γ-Alumina (γ-Al_2O_3, Aldrich), silica gel (Aldrich) or titania (Aldrich) and stirring for 2 hrs using a magnetic stirrer at room temperature (20 ± 1 °C) and ageing at room temperature for overnight [14]. The excess water is removed by heating the mixture on water bath and using a rota-vapor under mild vaccum to evaporate the water. The catalyst material is dried in an oven at 100 °C and 140 °C for 12 h. [15].

2.2. Instrumentation

2.2.1. Surface area analyzer

BET surface area of V_2O_5 loaded metal oxide catalysts was measured by nitrogen physisorption isotherms at 200 °C using the standard multipoint method on a Micrometrics ASAP 2020 (Micrometrics, USA), fully automatic, multi-point BET surface area analyzer under liquid N_2. Prior to the analysis samples were degassed in a stream of nitrogen at 473 K for 24 h.

2.2.2. Temperature programmed desorption (TPD)

In the TPD experiments, the catalyst was pretreated at 350 °C under the stream of helium which was used as a carrier flowing at 60 mL/min for 60 min and the temperature was thereafter brought down to 80 °C. A 4.1% ammonia in helium gas mixture was passed (30 mL/min) over the catalyst for 60 min. The excess ammonia was removed by passing helium with a flow rate of 30 mL/min over the catalyst for 30 min. The temperature was raised gradually to 950 °C by means of a temperature ramp of 10 °C/min under the flow of helium and the desorption was recorded.

2.2.3. FT-IR spectroscopy

FT-IR spectroscopy of catalyst samples was carried out on a Perkin Elmer BX model spectrometer in the 400–4000 cm^{-1} region using the KBr disc technique. Dry KBr was added to the samples and thoroughly homogenized. Transparent discs were formed and analyzed for IR spectral measurements.

2.2.4. Elemental analysis

The elemental composition of the catalysts was determined by ICP-OES using an Optima 5300 DV PerkinElmer optical emission spectrometer, showed that the experimental values were in close agreement with the theoretical values confirming the composition of the materials and adsorption of the V_2O_5 on the three supporting materials.

2.2.5. SEM studies

The SEM images summarize the main features of the prepared catalysts. Magnification of micrographs ranges from 1200× to 3500× with accelerator voltages at 12 kV and 20 kV. All samples were viewed in a Phillips XL30 electron scanning microscope interfaced with EDAX version 3.2.

2.2.6. XRD studies

X-ray diffraction analyses were performed to characterize of the catalyst. The powder diffraction patterns were recorded by X-ray diffraction using a Bruker AXS, D8 advance diffractometer with Cu

Table 1
BET surface area and acidity of V_2O_5 loaded supports ($n = 2$).

Catalyst (%)	Surface area (m^2/g)	Acidity (mmol NH_3/g)	Specific acidity (mmol NH_3/m^2)
γ-Al_2O_3	210	850	4.05
SiO_2	165	3800	23.0
TiO_2	41	558	13.6
V_2O_5	20	2543	127.6
1% V_2O_5/Al_2O_3	192	920	4.8
5% V_2O_5/Al_2O_3	175	1250	7.1
1% V_2O_5/SiO_2	142	3920	27.6
5% V_2O_5/SiO_2	104	4250	40.8
1% V_2O_5/TiO_2	39	610	15.6
5% V_2O_5/TiO_2	36	785	21.8

Kα radiation with wave length 0.15406 nm at 40 kV and 30 mA. Data was collected over the range 10–90° with a step size of 0.5/s.

2.2.7. GC–MS analysis

In all the experiments the organic layer was extracted by using 3×5.0 mL diethyl ether in a separating funnel and excess water was removed by the addition of anhydrous sodium sulfate (Na_2SO_4). The product was filtered and the solvent is allowed to evaporate. The product was characterized by GC and GC–MS. The amount of DCB was consumed in the reaction are expressed as a percentage of original amount and it referred reaction conversion. % Selectivity refers to the amount of product formed divided by the reactant consumed.

3. Results and discussion

3.1. Brunauer–Emmett–Teller surface area analysis (BET)

Ni and V_2O_5 loaded on Al_2O_3 and TiO_2 support material exhibited a lower surface area than silica supported catalysts. Surface area decreased with 5% loading of V_2O_5 on both Al_2O_3 and TiO_2 (Table 1). Pure vanadia has lower BET surface area and with 1 wt% V_2O_5 loading, most of the pores of Al_2O_3 and TiO_2 get occupied. When the % loading of V_2O_5 increase to 5% all the pores occupied by V_2O_5 and forming layers on the surface of metal supports and decreases the total surface area. This is also confirmed with the SEM images (Fig. 2). The loading of V_2O_5 on silica also exhibited decrease in surface area. Also during the impregnation stage in the preparation, surface hydroxyl groups of the silica get consumed by reaction with the active phase precursor. Such a surface reaction may be caused the decrease of surface area [15,16].

3.2. Temperature programmed desorption (TPD)

The TPR results show that as the % vanadia loading increased, the acidity as measured by mmol of ammonia adsorbed enhanced. As vanadium pentoxide is an acidic catalyst, it further enhances the acidity of support. As a result of decrease in surface area of the catalyst with increased loading of vanadia, the specific acidity of the loaded catalyst increases with vanadia loading. Among the three catalysts, silica supported catalyst is proved to be highly acidic in nature, followed by alumina and titania with lower acidity.

3.3. Fourier transform infrared spectroscopy (FT-IR)

A distinct absorption band at 1020 cm^{-1} observed with 5% V_2O_5/Al_2O_3 and a shoulder with 1% V_2O_5/Al_2O_3 is not observed in the IR spectrum of pure Al_2O_3 can be attributed to V=O vibrational stretching arising from the presence of V_2O_5 [17]. The stretching vibration of hydroxyl groups also appeared at 1630 cm^{-1} and 3462 cm^{-1} and 3467 cm^{-1} (supplementary materials Fig. S1a and b) [18,19]. IR spectra of 1% and 5% V_2O_5/SiO_2 catalysts (supplementary materials Fig. S1c and d) show absorption bands at 1095 and 1099 cm^{-1} (asymmetrical Si—O—Si). The vibrational stretching frequency of the hydroxyl group appears at 3435 cm^{-1}. The Si—O—Si bond which is observed at 1095 cm^{-1} and 1099 cm^{-1} is probably overlapping with the V=O absorption band which is expected for V_2O_5 at approximately 1020 cm^{-1} [17]. The absorption band at 1020 cm^{-1} with 5% V_2O_5/TiO_2 shows V=O vibrational stretching which can be attributed to the presence of V_2O_5. The two bands at 539 cm^{-1} and 675 cm^{-1} is due to presence of TiO_2 [17]. The absorption bands at 1639 cm^{-1} and 3462 cm^{-1} 1% V_2O_5/TiO_2 as well as 3462 cm^{-1} can be assigned to the hydroxyl group vibrational stretching. (supplementary materials Fig. S1e and f).

3.4. Scanning electron microscopy (SEM)

In the presence of V_2O_5 (white glow) on Al_2O_3 surface is noticeable in Fig. 2a and becomes more conspicuous in Fig. 2b as it seems to totally occupy the pores As observed from Fig. 2c, V_2O_5 is distributed over silica surface. An increase to 5% V_2O_5 loading (Fig. 2d) showed that V_2O_5 particles are closer together and occupy the surface more densely consistent with BET results. From Fig. 2e, it is shown that V_2O_5 (white fluffy substance) is evenly dispersed on the surface of titanium dioxide. When V_2O_5 loading is increased to 5% (Fig. 2f), the pores of TiO_2 appear to be completely occupied. Wide distribution of small particles over support material is observed with 1% V_2O_5 loading. With an increase from 1 wt% to 5 wt% V_2O_5 loading, Al_2O_3 and TiO_2 surfaces seem to be completely occupied with V_2O_5. For silica, the V_2O_5 particles are closer together but much of the surface is still visible (Fig. 2d). A possible reason could be that silica has a large surface area and therefore requires more V_2O_5 particles to occupy its pores. The SEM images confirm the crystalline nature of the catalysts, which is not affected by the different loadings of vanadia.

3.5. X-ray diffraction (XRD)

Fig. S2a and b exhibits XRD patterns for V_2O_5/Al_2O_3 catalyst. X-ray diffraction peaks for V_2O_5 and Al_2O_3 are identified and are consistent with literature [20,21]. The XRD patterns for V_2O_5/SiO_2 catalyst are exhibited in Fig. S2c and d. The characteristic peak of SiO_2 appears at $2\theta = 22°$ [17]. X-ray diffraction peaks for V_2O_5 are identified in agreement with literature reported data [22,23]. The XRD patterns for V_2O_5/TiO_2 catalyst are illustrated in Fig. S2e and f. The presence of crystalline V_2O_5 phase is evident in the catalyst while the presence of VO_2 phase is manifested with an increase in wt% of V_2O_5. X-ray diffraction peaks for TiO_2 are also identified [24].

3.6. Product identification

All the experiments were carried out under the controlled conditions of room temperature (20 ± 1 °C) using 20 mL aqueous solution

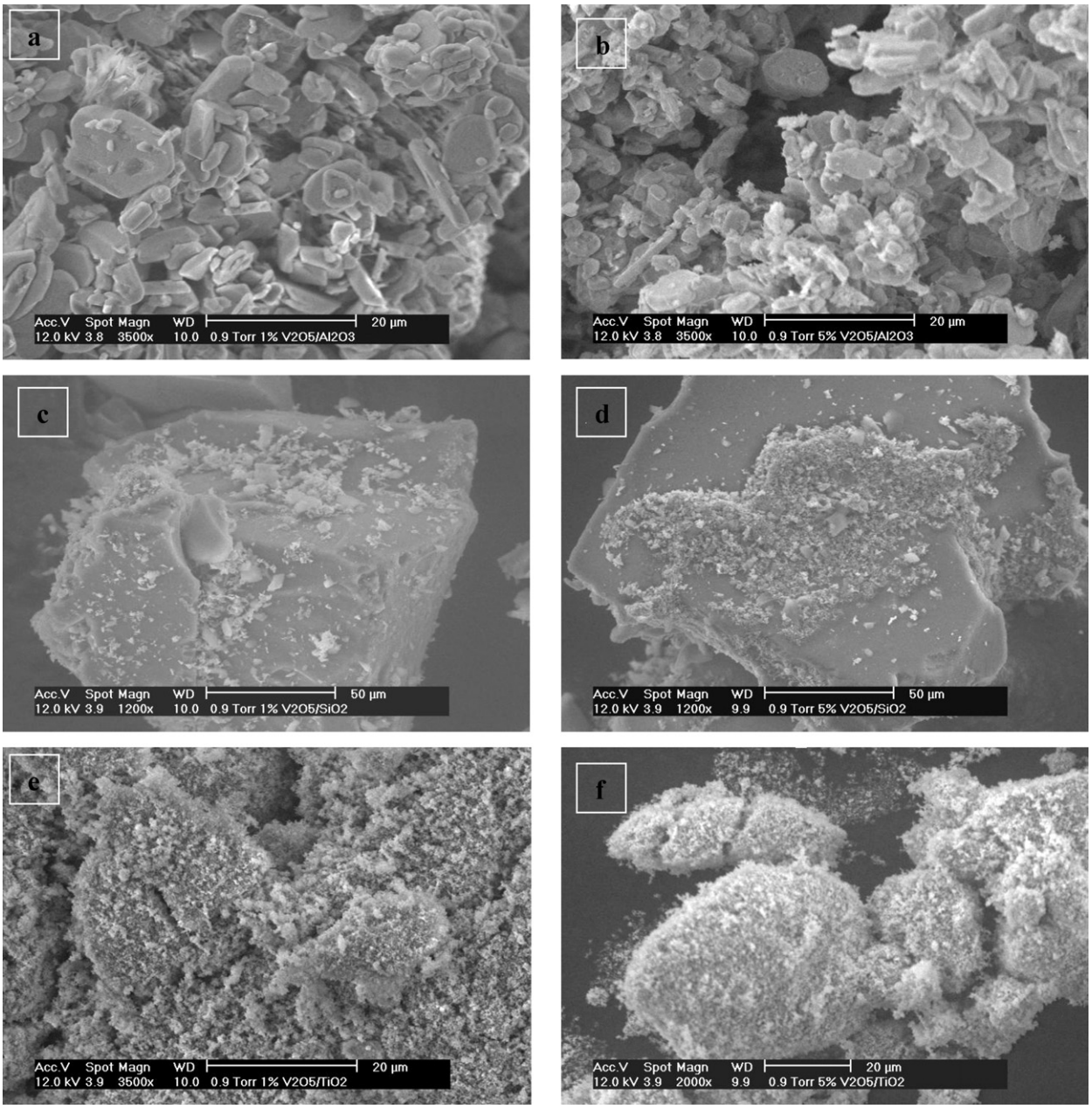

Fig. 2. SEM images: (a and b) 1% V_2O_5 and 5% V_2O_5 on Al_2O_3 support; (c and d) 1% V_2O_5 and 5% V_2O_5 on SiO_2 support; and (e and f) 1% V_2O_5 and 5% V_2O_5 on TiO_2 support.

10% (v/v) of 1,2-dichlorobenzene (DCB) at fixed ozone concentration and flow rate. All reactions were done in duplicate or triplicate. Conversion and selectivity was calculated for all reactions [25]. The ozonation experiments were conducted by aerating the samples with ozone enriched with oxygen for different time intervolves, viz. 2, 4 and 5 h and found that no reaction occurred with the oxygen. After ozone aeration, the organic portion of the reaction mixture was extracted and analyzed the products at each reaction. The two major products during reaction progress for the reactions were identified by GC/GC–MS (Fig. 3) and confirmed that 3,4-dichloro-5-hydroxy-2(5H)-furanone (DHF) and mucochloric acid (MCA) (Fig. 4) based on the mass spectra and the reference standard. Furthermore, the IR spectrum of the main product, MCA showed absorption band at 1782 cm^{-1} which can be assigned to the C=O bond. The C—H stretching is observed at 898 cm^{-1}, 1079 cm^{-1} and 2866 cm^{-1}. The OH vibrational stretching appeared at 3055 cm^{-1}.

The functional groups observed in the IR spectrum are in good agreement spectrum corresponding to MCA. Further the qualitative (lime water) test confirmed the release of CO_2 during the ozonation reaction and suggesting the mineralization of DCB. Literature reports suggest that ozonation of organic compounds in water produces more biodegradable oxygenated organic products and low molecular weight acids [26]. The unidentified products (UnP) may constitute some aldehydes, small carboxylic acids and ketones [27]. Thus, for mass balance and carbon accountability, for each mole of DHF or MCA formed (which contain 4C), two moles of CO_2 is possibly generated. In the conversion and selectivity tables, CO_2 is not included. Mucochloric acid is largely used as an intermediate in making dyes, pigments, pesticides and pharmaceuticals. This substance has no potential for bioaccumulation and is partially biodegradable [28], with prolonged ozonation, DHF was found to tautomerize to MCA. MCA is capable of undergoing ring–chain tautomerism, and its molecule possesses several reaction centers [29].

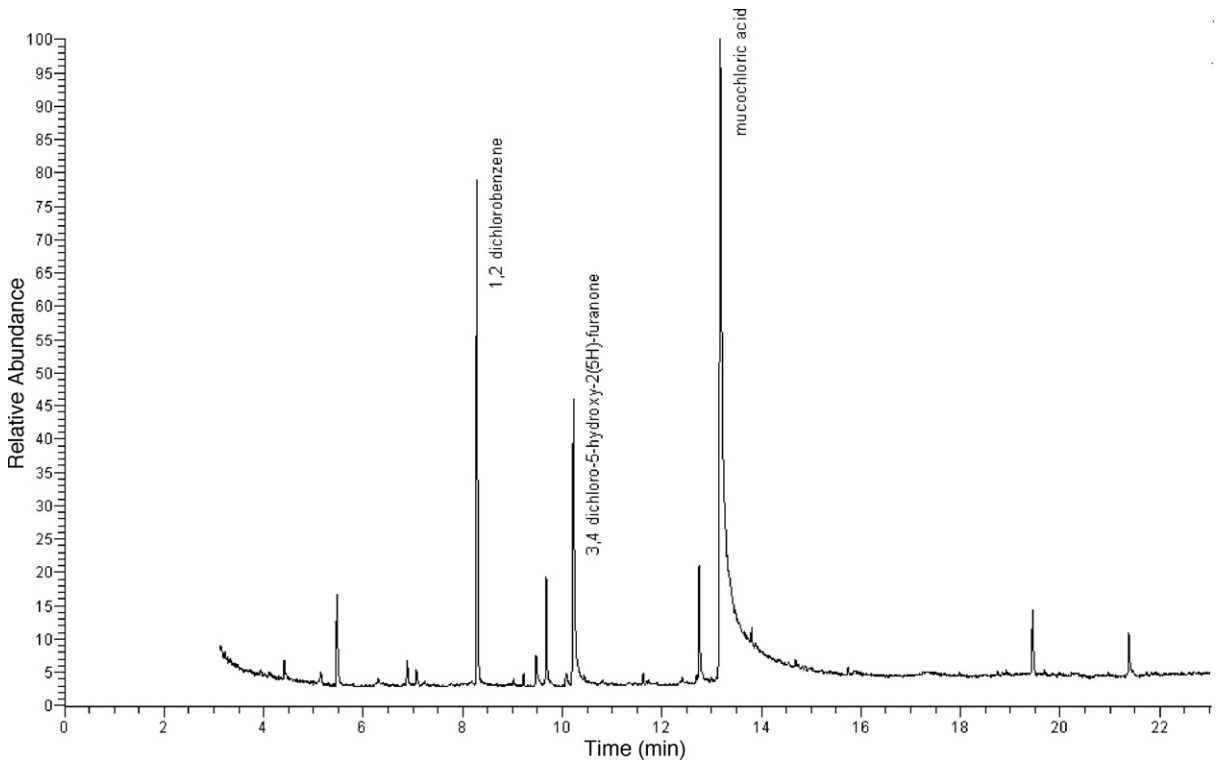

Fig. 3. GC–MS chromatogram of product mixture.

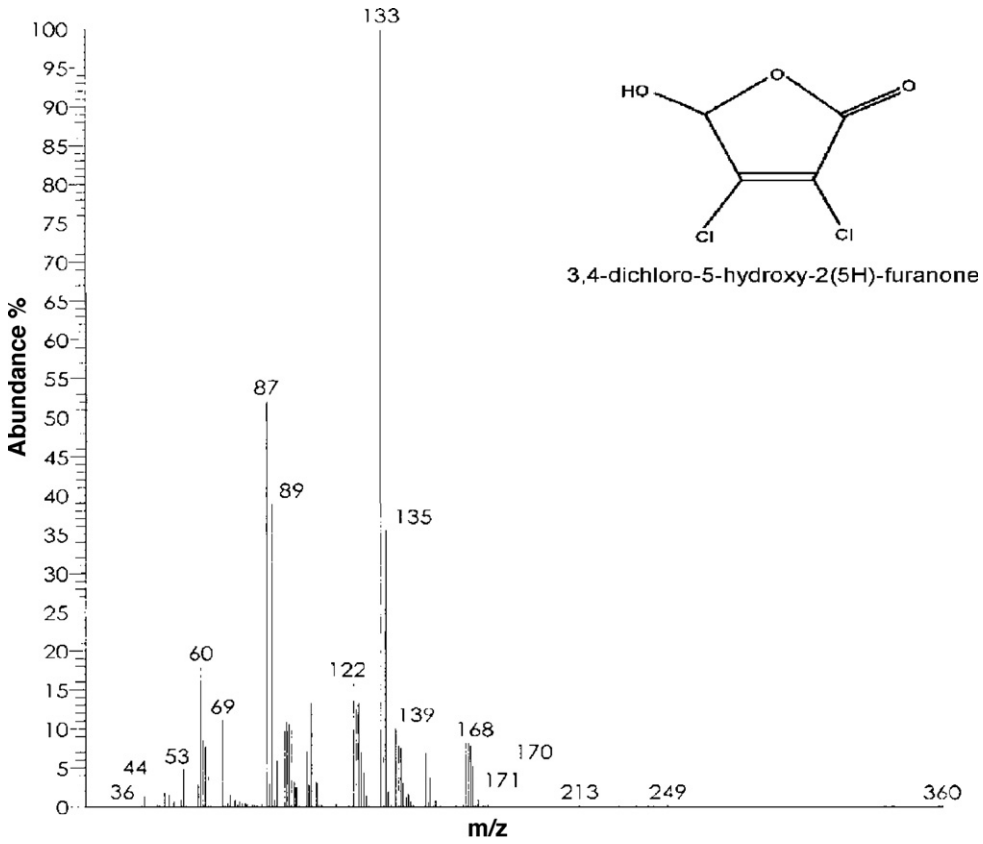

Fig. 4. Mass spectrum of mucochloric acid (MCA).

Table 2
% Conversion of DCB after 2 h ozonation in presence of 5% (w/w) vanadium pentoxide loaded catalysts (0.2 g/20 L 10%, v/v DCB) at pH 5.0, 7.0 and 11.0.

pH	% Conversion		
	V_2O_5/Al_2O_3	V_2O_5/TiO_2	V_2O_5/SiO_2
5	61.3	82.0	79.5
7	75.6	86.8	85.5
11	73.9	84.3	81.3

Table 3
Percentage conversion of DCB and product selectivity for ozonation reactions of at pH 7.0. Reaction mixture = 20 mL (10%, v/v of DCB in water); catalyst = 0.20 g/20 mL. Flow rate = 1 L/min. [O_3] = 1.094 mg/L. Temperature (20 ± 1 °C) (n = 2).

Ozonation time/h	Conversion %	% Selectivity		
		DHF	MCA	UnP
Uncatalyzed				
2	34.4	37.5	50.0	12.5
4	63.3	21.2	70.6	8.2
5	94.3	9.4	87.9	2.7
Catalyst: Al_2O_3 only				
2	73.6	45	35	20
4	94.4	27.3	44	28.7
5	96.8	11.8	58.1	30.1
Catalyst: SiO_2 only				
2	80.2	40	36	24
4	89.9	23.7	46.9	29.4
5	99.4	15.7	64.8	19.5
Catalyst: TiO_2 only				
2	75.4	17.5	40	42.5
4	89.5	12	54	34
5	90.9	8.9	57.8	33.3
Catalyst: V_2O_5 only				
2	70.1	16.7	43.3	40.0
4	90.9	14.8	55.5	29.7
5	91.6	11.8	60.0	28.2

In the recent times, it has attracted considerable attention as an accessible starting material, as it may be regarded as α,β-unsaturated acid, α,β-unsaturated aldehyde, tetra substituted Z-olefin, vinyl halide, latent hemiacetal, or pseudolactone [30] (Scheme 1).

3.7. Conversion and selectivity

To optimize the pH of the reaction, ozonation experiments were conducted with 10% (v/v) of 1,2-dichlorobenzene dichlorobenzene, at pH 5, 7 and 11 in presence of 5% V_2O_5 loaded on three oxide supports (Table 2). A perusal of % conversion data in Table 2 indicates that optimum pH for DCB degradation for all three catalysts is pH 7. Hence the further catalyzed ozonation studies were performed at neutral pH.

3.7.1. Effect of metal oxides on DCB ozonation

The results of % conversion of DCB and selectivity toward products for the uncatalyzed ozonation and in presence of standalone alumina, silica, titania or vanadium pentoxide are summarized in Table 3. A perusal of data in Table 3 show that after 2 h ozonation, the % conversion with standalone metal oxides was higher compared to 34.4% with uncatalyzed reaction, i.e. with alumina

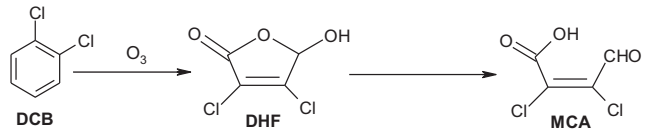

Scheme 1. 1,2-Dichlorobenzene (DCB); 3,4-dichloro-5-hydroxy-2(5H)-furanone (DHF) and nucochloric acid (MCA).

Table 4
Percentage conversion of DCB and product selectivity for ozonation reactions of at pH 7.0. Reaction mixture = 20 mL (10%, v/v of DCB in water); V_2O_5 = 0.20 g/20 mL. Flow rate = 1 L/min. [O_3] = 1.094 mg/L. Temperature (20 ± 1 °C) (n = 2).

Ozonation time/h	Conversion %	% Selectivity		
		DHF	MCA	UnP
Catalyst: 1% V_2O_5 on Al_2O_3				
2	72.8	51.6	35.5	12.9
4	94.2	27.6	45.3	27.1
5	100	0	100	0
Catalyst: 5% V_2O_5 on Al_2O_3				
2	75.6	36.8	39.3	23.9
4	96.1	30.5	55.7	13.8
5	99.7	0	100	0
Catalyst: 1% V_2O_5 on SiO_2				
2	80.4	40.0	36.0	24.0
4	90.9	21.9	52.5	25.6
5	99.7	0	100	0
Catalyst: 5% V_2O_5 on SiO_2				
2	85.5	23.3	56.7	20.0
4	95.9	23.7	59.6	16.7
5	99.6	0	100	0
Catalyst: 1% V_2O_5 on TiO_2				
2	74.7	38.3	34	27.7
4	90.8	25.2	47.3	27.5
5	99.6	0	97.1	2.9
Catalyst: 5% V_2O_5 on TiO_2				
2	86.8	50.0	40.0	10.0
4	93.5	24.3	47.7	28.0
5	99.7	0	100	0

(73.6), silica (80.2), titania (75.4) and vanadia (70.1) (Fig. 5a). After 4 h ozonation, relative to uncatalyzed (63.3%), metal oxides had improved conversions, viz. alumina (94.4), silica (89.9), titania (89.5) and vanadia (90.9) (Fig. 5b–e). Silica exhibited higher % conversion compared to other catalysts and reached 99.4% after 5 h. After 5 h ozonation, relative to uncatalyzed ozonation, except silica, the % conversion was lower with other oxides materials alone, but the selectivity toward products varied significantly. Interestingly, all the metal oxide catalyzed reactions had higher % of unidentified products and lower % MCA, relative to the uncatalyzed reaction. The profiles of reaction products in Fig. 5 evidently indicates that for all reactions, during initial period of ozone aeration, the concentration of MCA was low and DHF and other unidentified products were high. With prolonged ozonation the amount of MCA always increased, while the DHF and UnP were either in steady state or decreased. This clearly suggests that with further ozonation, DHF and some of UnP may get transformed to MCA, resulting in MCA as the main product in all reactions.

3.7.2. Ozonation reactions with mixed oxide catalysts

Table 4 summarizes the results of percentage conversion and selectivity toward six catalysts with 1% and 5% V_2O_5 loaded on three different metal oxide supports. The conversion and selectivity efficiencies with different loadings of vanadia on metal oxide supports are illustrated in Fig. 6a–f. After 2 h ozonation, while 5% vanadia loaded catalysts registered higher conversion than the 1% loaded, but for both the efficiency conversion was in the order with $SiO_2 > Al_2O_3 > TiO_2$. The 1% V_2O_5/Al_2O_3 and 5% V_2O_5/TiO_2 yielded higher DHF in the first 2 h. After 5 h ozone aeration, the trend remained the same, the conversions with 1% V_2O_5/Al_2O_3, 1% V_2O_5/SiO_2 and 1% V_2O_5/TiO_2 catalysts were 100%, 99.7% and 99.6% respectively and yielding 100%, 100% and 97.1% selectivity toward MCA (Fig. 6a, c and e), With 5% V_2O_5/Al_2O_3, 5% V_2O_5/SiO_2 and 5% V_2O_5/TiO_2 catalysts, the conversions were 99.7%, 99.6%, and 99.7% respectively and selectivity toward MCA was 100% in all three systems, which is a distinction from the uncatalyzed or single metal oxides catalyzed reactions (Fig. 6b, d and f). The BET analysis of catalysts revealed that surface areas were in the order

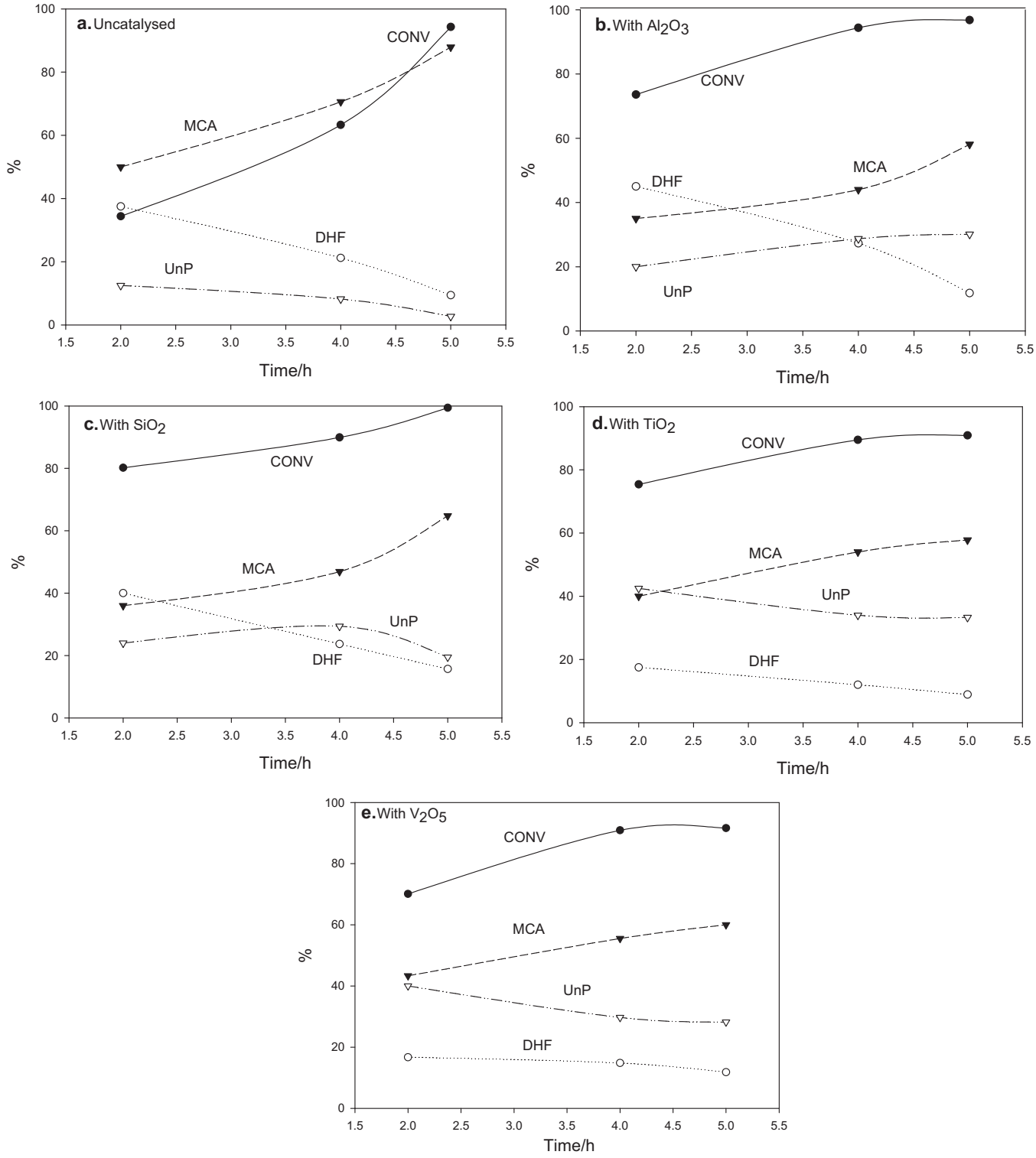

Fig. 5. Percentage conversion of DCB and product selectivity for ozonation reactions of at pH 7.0 (uncatalyzed, in presence of Al_2O_3, SiO_2, TiO_2 or V_2O_5 as catalysts. Reaction mixture = 20 mL (10%, v/v of DCB in water); catalyst = 0.20 g/20 mL; flow rate = 1 L/min. [O_3] = 1.094 mg/L; temperature (20 ± 1 °C) ($n = 2$).

of $V_2O_5/SiO_2 \gg V_2O_5/TiO_2 > V_2O_5/Al_2O_3$ (Table 1). Catalyst activity seems to be independent of catalyst surface area, as % conversion and selectivity were of similar magnitude in all three cases, pointing that activity is resultant of the combination of active sites of vanadium and support material.

Studies by Ernst et al. [31] revealed that the catalyst exhibit different adsorption abilities to different model compounds and that the adsorption of organic model substances on the catalyst's surface. Although hydroxyl groups are present on all metal oxides surfaces, the amount and the properties of the hydroxyls depend

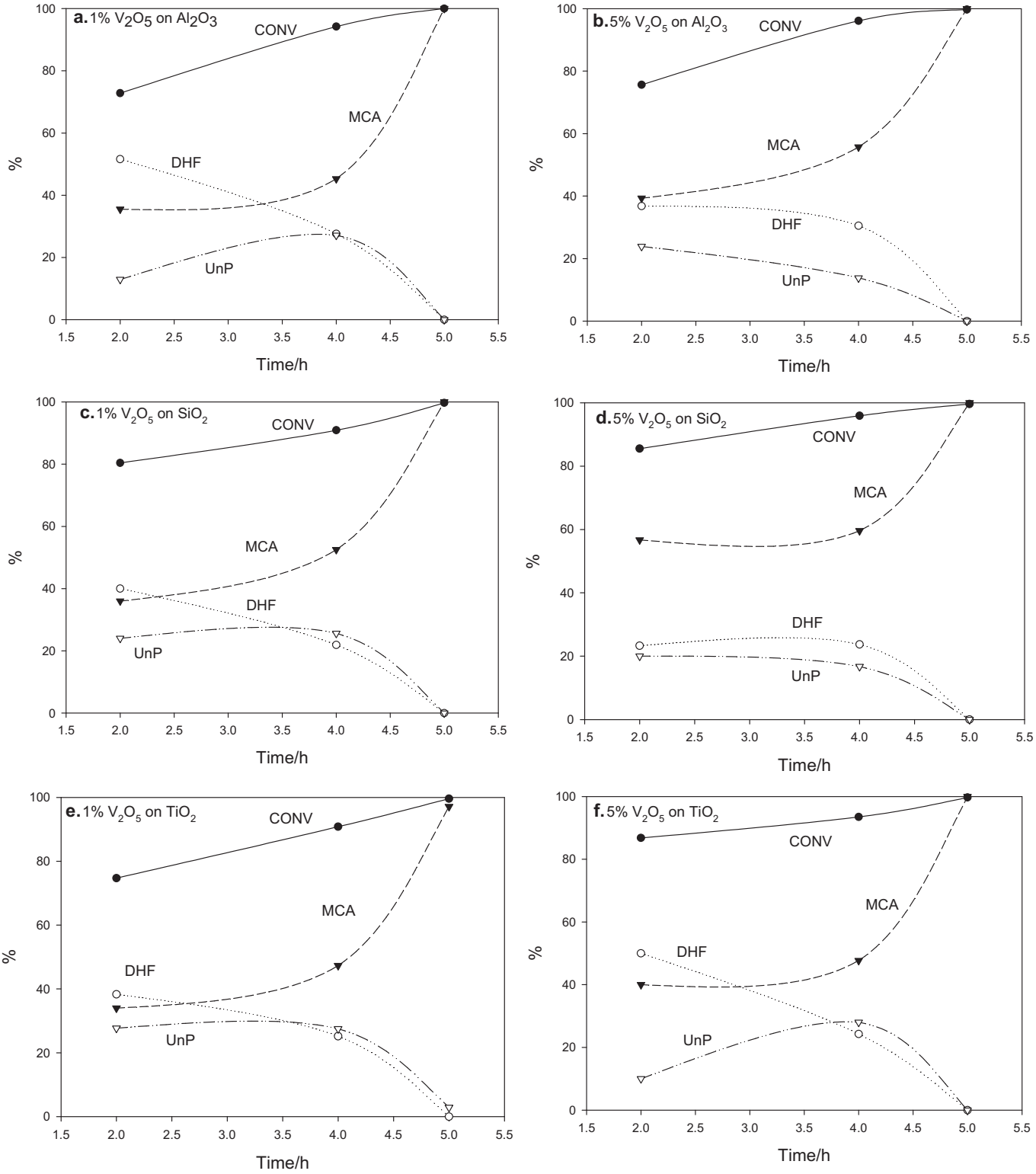

Fig. 6. Percentage conversion of DCB and product selectivity for ozonation reactions of at pH 7.0 (with 1% V_2O_5/Al_2O_3, 5% V_2O_5/Al_2O_3, 1% V_2O_5/SiO_2, 5% V_2O_5/SiO_2, 1% V_2O_5/TiO_2 or 5% V_2O_5/TiO_2). Reaction mixture = 20 mL (10%, v/v of DCB in water); catalyst = 0.20 g/20 mL; flow rate = 1 L/min. $[O_3]$ = 1.094 mg/L; temperature (20 ± 1 °C) (n = 2).

on the metal oxide. The main parameter, which determines the catalytic properties of metal oxides, is acidity and basicity. The hydroxyl groups formed at metal oxide surface behave as Brönsted acid sites. Lewis acids and Lewis bases are sites located on the metal cation and coordinatively unsaturated oxygen, respectively. Both Brönsted and Lewis acid sites are thought to be the catalytic centers of metal oxide. The chemistry of alumina and titania differs significantly from that of silica. As opposed to silica,

alumina and titania are capable of both ion and ligand exchange. Resulting from low pH of point of zero charge, silica is capable only of cation exchange. Furthermore, titania and alumina, as opposed to silica, have Lewis acid sites on their surface, which are responsible for the ligand exchange ability of these oxides [32].

The support serves three important functions in the catalytic system, i.e. to increase the surface area of the metal or metal oxide by providing a matrix that enables their dispersion as very small particles, to restrain the sintering of the active catalyst material and to improve its hydrophobic nature and its thermal, hydrolytic, and chemical stability. Yurii et al. in their study reported the efficiency of supports as CeO_2 > alumina > NaY zeolite > ZrO_2 > TiO_2 [33], They have reported that the efficiency of oxides as support materials for metal ion catalyst loading for ozone decomposition as SiO_2 > Al_2O_3 >SiO_2-Al_2O_3 > TiO_2, which fairly agrees with the results observed in the current study with three oxide materials as supports. During the studies on conversion of pentanes to phthalic and maleic anhydrides with oxygen, Singh et al. have reported good conversion and selectivity toward the products, when V_2O_5 loaded on hydroxyapatite was used as catalyst compared to support or V_2O_5 alone [22].

A review of the literature on the ozone decomposition kinetics in aqueous solutions, the most common observation is the reported disagreement among different researchers as to both the order of the decomposition reaction and the magnitude of the reaction rate constant. Although, it is generally agreed that the reaction is catalyzed by the hydroxide ion, there are also substantial differences regarding the pH dependence of the reaction. While the rate constant increased with increase in hydroxide ion concentration, the decomposition of ozone can be approximated by a second-order reaction in the pH range 2–9.5 [34]. It is reported that while direct decomposition of ozone is main path under acidic conditions (pH 5 and below), both direct decomposition and hydroxide ion initiated path have similar magnitude under alkaline conditions (pH 9 and above), and at neutral pH direct decomposition is reported to be about 50 times faster than OH^- facilitated decomposition [35]. The water's reactivity toward ozone changes substantially as ozonation depletes the readily reactive compounds. According to Crittenden et al., the overall rate of ozone decay in water is generally consistent with first order kinetics, although the decay of ozone in some waters does not always follow this uniform first order decay model [36]. Lin et al. have investigated the activities of a series of oxide supports and dozens of supported metal catalysts toward the decomposition of aqueous ozone. While Al_2O_3, SiO_2, $SiO_2{\cdot}Al_2O_3$ and TiO_2 have showed no or negligible activity, five noble metals and many other metals loaded on supports exhibited high activity (mg O_3 min^{-1} g^{-1} catalyst) in the order M/SiO_2 (0.22), M/Al_2O_3 (0.16) and M/TiO_2 (0.09) and M/$SiO_2{\cdot}Al_2O_3$, and rate constants in parenthesis values are for M is Ni. They reported that decomposition rate of ozone on supported metal oxide catalysts depended on four parameters namely, adsorption ability of O_3, decomposition ability of O_3, activity of oxygen species and desorption ability of O_2 on the catalyst surface [37]. Radhakrishnan et al. have reported the rate of ozone decomposition for MnO_2 loaded on oxide supports followed the trend: Al_2O_3 > ZrO_2 > TiO_2 [38]. During the gas phase oxidation of methanol and total reduced sulfur compounds with ozone over V_2O_5/TiO_2 catalyst, the presence of humidity reportedly facilitated the oxidations [39]. While reviewing the work on catalytic removal of NO, Parvulescu et al. have reported that the order of activity for supported vanadia is TiO_2-SiO_2 > γ-Al_2O_3 > SiO_2 [40]. As per the acidity scale for binary oxides from thermo-chemical data for oxo acid salts, the values for MgO, Al_2O_3, TiO_2, SiO_2, and V_2O_5 are −4.5, −2.0, 0.7, 0.9, and 3.0, respectively; the lower the value the larger the basicity of the oxide, thus vanadia remains most acidic oxide [41].

During oxidation of carbon black with $^{18}O_2$ at 625–675 K, in a high-vacuum batch reactor using V_2O_5 as catalyst, no oxygen exchange between $C^{18}O_2$ and V_2O_5 reported to occur. Quite some lattice oxygen of V_2O_5 was incorporated in the carbon oxides produced [42]. The oxidation reactions over combinations of two metal oxides have been explained by a spill-over mechanism. Oxygen is adsorbed and activated on one metal oxide (the donor) and transferred to the second metal oxide (the acceptor). The reactant (e.g., a hydrocarbon) reacts with the oxygen adsorbed on the acceptor.

During the oxidation of limonene using vanadia on titania, the activity of the V_2O_5/TiO_2 is often related with the solid acidity. Both Lewis and Brönsted acid sites may be present as it was determined by IR of adsorbed pyridine. However, when diluted t-BHP is used as oxidant, only the samples bearing vanadia on the particles outer surface are active. This means that limonene oxidation takes only place on the vanadium sites. Oxidation of methanol into formaldehyde proceeds selectively on the MoO_3 monolayer, which covers the surface of all the supports. Reportedly methanol is selectively adsorbed on the Brönsted acid site as methoxide, and then oxidized into formaldehyde as a result of dehydrogenation by neighbored oxygen [43].

It is ascertained that supporting vanadium oxides on TiO_2-anatase leads to very active oxidation catalysts, more active than those obtained with other supports. This has also been found for V_2O_5-TiO_2 (anatase) "monolayer" type catalysts for the selective oxidation of ortho-xylene to phthalic anhydride. The reason for this activity enhancement can be found on the good dispersion of vanadium oxide on TiO_2 giving rise to "isolated" vanadyl centers and "polymeric" polyvanadate species, possibly of the metavanadate-type, and also on the semiconductor nature of TiO_2, whose conduction band is not very far from the d-orbital levels of vanadyl centers, located in the energy gap [44]. Having an insight into the mechanism of reaction between ammonia and nitric oxide, all authors agree in indicating that ammonia adsorbs on pure V_2O_5, on V_2O_5-TiO_2, on V_2O_5/SiO_2-TiO_2, etc. in two different strongly held species as (i) molecularly adsorbed ammonia, through a Lewis-type interaction on coordinately unsaturated cations; and (ii) ammonia adsorbed as ammonium ions, over Brönsted acidic —OH surface hydroxyl groups. Soe et al. from their studies on V_2O_5 impregnated on TiO_2 support reported the existence of V^{4+} and V^{3+} besides V^{5+}. That is, vanadium has a stable pentavalent oxidation value, but it forms V^{3+} through oxygen combination, and it is known that activation energy was much lower in vanadia containing V^{3+} than vanadia, where V^{5+} is dominant. In titania in addition to Ti^{4+} state, small amount of Ti^{3+} and Ti^{2+} reportedly coexist [45].

For V_2O_5/SiO_2 catalysts prepared by grafting or wet precipitation methods, the number of acid sites increased with increase in vanadium loading (1–20%) [46]. On alumina, at low V coverage, a large part of the vanadate layer is bound to acid-base pairs of alumina. At low V coverage, <3% V_2O_5 the acidic character of V_2O_5/Al_2O_3 catalyst can be ascribed to V free alumina, whereas at higher vanadium coverage, it is largely attributed to vanadate compounds [47]. During the ethane dehydrogenation studies it is reported that the lattice oxygen migration to react with ethane requires less energy on the V_2O_5/Al_2O_3 catalyst. Thus, lattice oxygen mobility is improved. Deposition of V_2O_5 on alumina and titania supports gave rise to catalysts with lower number of acid sites than the respective supports, while for samples prepared on silica, an increase in acid sites was observed after V_2O_5 deposition [48]. VO species on the support centers act as electron attractor centers creating Lewis like V species. The TiO_2-anatase supports, if pure only show Lewis acidity, whereas in presence of water, V—O—H is formed. Thus, vanadyl sites are Lewis acidic and can convert to Brönsted sites by water adsorption [49].

Analogous to the mechanism proposed by Rosal et al., in the present study it is proposed that the dissolved ozone adsorbs and decomposes on the surfaces of metal oxide support, the resulting radicals being responsible for indirect oxidation reactions. Besides the liquid phase reaction of surface-produced radicals, the adsorption of organic molecules on the catalyst surface (vanadia, strongly acidic site) leads to additional mechanisms: an adsorbed organic compound may be attacked by molecular ozone or radicals from the bulk aqueous phase or with an adsorbed ozone molecule on adjacent active site (oxide support) or the products of surface ozone decomposition. The formation of surface oxidation sites or the adsorption of neutral compounds on oxides is difficult in aqueous solutions due to the competitive adsorption of water molecules. Adsorption is easier for ionizable organic compounds in water, if the surface is charged allowing ion exchange. In fact, the surface of metal oxides exhibits ion exchange properties and the hydroxyl groups formed behave as Brönsted acid sites and dissociate depending on the pH of the solution [50].

The observed optimum condition for the reaction, pH 7 supports the reported nearer point of zero charge, where the oxide active sites are marginally charged facilitating the adsorption of organic substrate. [32]. Near pH 7, direct decomposition rate of ozone is about 30–50 times higher than the OH^- ion initiated decomposition. Effective ozonation at pH 7 could possibly be explained by the fact that the products which are formed as a result of degradation as well as the parent compound itself are attacked simultaneously, both becoming important scavengers of hydroxyl radicals [51]. Also, besides AOPs being compound specific, it is important to note that a high production of •OH radicals can even lead to a lower reaction rate because the radicals recombine and are not useful for the oxidation process [52]. The efficiency of the catalytic ozonation process depends to a great extent on the catalyst and its surface properties as well as the pH of the solution that influences the properties of the surface active sites and ozone decomposition reactions in aqueous solutions [53]. The observed efficiency of vanadia on the metal oxide supports, $SiO_2 > Al_2O_3 > TiO_2$ agreed well with the ozone decomposition efficiencies for Ni on the same supported oxides reported by Lin et al. Further, TPD data for pure oxides and vanadia loaded on the three oxide supports in the current study are in agreement with the literature reported trends and specific acidities of the catalyst materials were in line with their observed catalytic efficiencies.

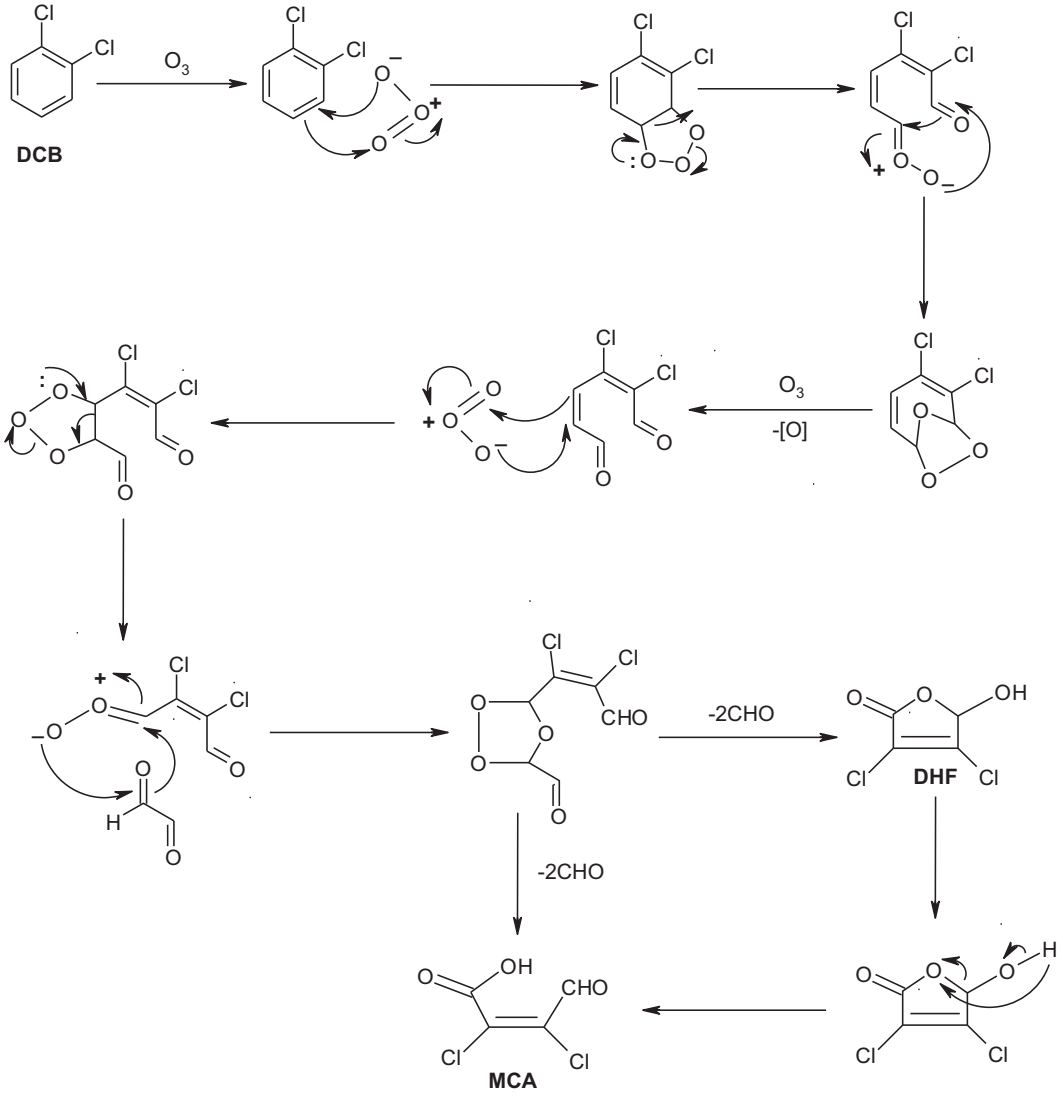

Mechanism of Scheme

Dichloro substituted benzene with electron withdrawing groups will be less reactive and the ozone molecule attacks mainly on the least deactivated meta position, leading to the formation of hydroxylated intermediate, which gets further oxidized. An ozonide is generated and added to the C=C double bond. The hydroxyl radicals (•OH) generated in the system attack the reaction intermediates to form DHF. Under oxidizing conditions, this intermediate undergoes rearrangement to form the final product mucochloric acid. In addition to the proposed mechanism scheme, the direct pathway for the formulation of MCA without going through DHF as an intermediate is not to be ruled out. That can possibly happen without the ring closure of DCB, after the ozone attack on the double bond and resulting in the opening of the six-membered ring.

4. Conclusions

Metal oxide supported V_2O_5 catalysts are found to have great product selectivity during the oxidation of 1,2-dichlobenzene by ozone in water at pH 7. While conversion efficiency of the support was $SiO_2 > Al_2O_3 > TiO_2$, for 2 h ozonation, 5% V_2O_5 loaded catalysts registered higher conversion than with 1% loaded. Main oxidation product, mucochloric acid was produced with (98–100%) selectivity and little mineralization.

Acknowledgments

Authors thank the National Research Foundation, Pretoria and the University of KwaZulu-Natal for the financial support and facilities.

Appendix A. Supplementary data

Supplementary data associated with this article can be found, in the online version, at doi:10.1016/j.apcatb.2012.01.004.

References

[1] C. Cooper, R. Burch, Water Res. 33 (1999) 3695–3700.
[2] R.J. Miltner, H.M. Shukairy, R.S. Summers, J. Am. Water Works Assoc. 84 (1992) 53–62.
[3] U. Iriarte, J.I. Alvarez-Uriarte, R. Lopez-Fonseca, J.R. Gonzelez-Velasco, Environ. Chem. Lett. 1 (2003) 57–61.
[4] B. Langlais, D.A. Reckhow, D.R. Brink, Ozone in Water Treatment, Applications and Engineering, Lewis Publishers, Inc., Chelsea, MI, 1991, pp. 569–584.
[5] M. Manassis, S. Constantinos, Ozone Sci. Eng. 25 (2003) 167–175.
[6] S.D. Richardson, A.D. Thruston, T.V. Caughran, P.H. Chen, T.W. Collette, K.M. Schenck, B.W. Lykins Jr., C. Rav-acha, V. Glezer, Water Air Soil Pollut. 123 (2000) 95–102.
[7] R. Song, P. Westerhoff, R. Minear, G. Amy, J. Am. Water Works Assoc. 89 (2007) 68–78.
[8] E. Gilbert, Water Res. 22 (1988) 123–126.
[9] J.H. Larsen, M. Lee, P.C. Frost, G.A. Lamberti, D.M. Lodge, Environ. Toxicol. Chem. 27 (2004) 676–681.
[10] M.D. Amiridis, R.V. Duevel, I.E. Wachs, Appl. Catal. B: Environ. 20 (1999) 111–122.
[11] Public Health Goals for 1,2 Dichlorobenzene in Drinking Water, California Public Health Goal (PHG), 1997, pp. 1–19. http://oehha.ca.gov/water/phg/pdf/12dcb_c.pdf (accessed January 2011).
[12] J.R. Utrilla, M. Sanchez-Polo, M.A. Mondaca, C.A. Zaror, J. Chem. Technol. Biotechnol. 77 (2002) 883–890.
[13] K. Rakness, G. Gordon, B. Langlais, W. Masschelein, N. Matsumoto, Y. Richard, C.M. Robson, I. Somiya, Ozone Sci. Eng. 8 (1996) 209–229.
[14] H. Einaga, S. Futamura, J. Catal. 227 (2004) 304–312.
[15] A. Rahman, V.S.R. Pullabhotla, S.B. Jonnalagadda, Catal. Commun. 9 (2008) 2417–2421.
[16] A. Saadi, R. Merabti, Z. Rassoul, M.M. Bettahar, J. Mol. Catal. 253 (2006) 79–85.
[17] R.A. Nyquist, R.O. Kagel, Infrared Spectra of Inorganic Compounds, vol. 135, Academic Press Inc., London, 1971, pp. 209–217.
[18] K. Nakamoto, Infrared Spectra of Inorganic and Coordination Compounds, 2nd edn., John Wiley and Sons, New York, 1990.
[19] S. Hong, M.S. Lee, S.S. Park, G. Lee, Catal. Today 87 (2003) 99–105.
[20] H. Yahiro, K. Nakaya, T. Yamamoto, K. Saiki, H. Yamaura, Catal. Commun. 7 (2006) 228–231.
[21] P.G. Savva, K. Goundani, J. Vakros, K. Bourikas, C. Fountzoula, D. Vattis, A. Lycourghiotis, C. Kordulis, Appl. Catal. B: Environ. 79 (2008) 199–207.
[22] S. Singh, S.B. Jonnalagadda, Catal. Lett. 126 (2008) 200–206.
[23] Y. Sato, T. Asada, H. Tokugawa, K. Kobayakawa, J. Power Sources 68 (1997) 674–679.
[24] Y. Hu, H.L. Tsai, C.L. Huang, Mater. Sci. Eng. A 344 (2003) 209–214.
[25] R.A. Sheldon, J.K. Kochi, Metal-Catalysed Oxidations of Organic Compounds: Mechanistic Principles and Synthetic Methodology Including Biochemical Processes, Academic Press, New York, 1981, pp. xvii–xix.
[26] F.J. Beltran, J.F. Garcıa-Araya, P.M. Alvarez, Environ. Prog. 19 (1) (2000) 28–35.
[27] R. Gerald, Chemosphere 28 (1994) 1447–1454.
[28] UNEP Publications, OECD, SIDS, Mucochloric Acid, 2003, pp. 1–10, http://www.chem.unep.ch/irptc/sids/oecdsids/87569.pdf (accessed January 2011).
[29] F. Bellina, C. Anselmi, F. Martina, R. Rossi, Eur. J. Org. Chem. 12 (2003) 2290–2302.
[30] J. Zhang, K.S. Das, T.T. Curran, D.T. Belmont, J.G. Davidson, J. Org. Chem. 70 (2005) 5890–5895.
[31] M. Ernst, F. Lurot, J.C. Schrotter, Appl. Catal. B 47 (2004) 15–25.
[32] B. Kasprzyk-Hordern, M. Ziółek, J. Nawrocki, Appl. Catal. B: Environ. 46 (2003) 639–669.
[33] Y.I. Matatov-Meytal, M. Sheintuch, Ind. Eng. Chem. Res. 37 (1998) 309–326.
[34] M.D. Gurol, P.C. Slnger, Environ. Sci. Technol. 16 (7) (1982) 377–383.
[35] J.L. Sotelo, F.J. Beltrln, F.J. Benitez, J. Beltrkn-Heredia, Ind. Eng. Chem. Res. 26 (1987) 39–43.
[36] J.C. Crittenden, R.R. Trussell, D.W. Hand, K.J. Howe, G. Tchobanoglous (Eds.), Water Treatment: Principles and Design, 2nd ed., John Wiley & Sons, New York, 2005.
[37] J. Lin, A. Kawai, T. Nakajima, Appl. Catal. B 39 (2002) 157–165.
[38] R. Radhakrishnan, S.T. Oyama, J.G. Chen, K. Asakura, J. Phys. Chem. B 105 (19) (2001) 4245–4253.
[39] E. Sahle-Demessie, V. Devulapelli, Appl. Catal. A: Gen. 361 (2009) 72–80.
[40] V.I. Parvulescu, P. Grange, B. Delmon, Catal. Today 46 (1998) 233–316.
[41] M. del Arco, M.J. Holgado, C. Marth, V. Rives, Langmuir 6 (1990) 801–806.
[42] G. Mul, F. Kapteijn, C. Doornkamp, J.A. Moulijn, J. Catal. 179 (1998) 258–266.
[43] M. Niwa, Y. Habuta, K. Okumura, N. Katada, Catal. Today 83 (2003) 213–218.
[44] G. Buscaa, L. Liettib, G. Ramisa, F. Berti, Appl. Catal. B: Environ. 18 (1998) 1–36.
[45] S. Phil-Won, L. Jun-Yub, S. Kyu-Seung, H. Sung-Ho, H. Sung-Chang, H. Suk-In, J. Hazard. Mater. 165 (2009) 39–47.
[46] D. Jackson, J.S.J. Hargreaves, Metal Oxide catalysis, vol. 1, Wiley-VCH, 2008, p. 430.
[47] J. Le Bars, J.C. Vedrine, A. Auroux, S. Trautman, M. Baerns, Appl. Catal. A 119 (1994) 341–354.
[48] J. Le Bars, A. Auroux, M. Forissier, J.C. Vedrine, J. Catal. 162 (1996) 250–259.
[49] G. Busca, L. Lietti, G. Ramis, F. Berto, Appl. Catal. B 18 (1998) 1–36.
[50] R. Rosal, A. Rodríguez, M.S. Gonzalo, E. García-Calvo, Appl. Catal. B: Environ. 84 (2008) 48–57.
[51] D. Vogna, R. Marotta, A. Napolitano, R. Andreozzi, M. Ischia, Water Res. 38 (2004) 414–422.
[52] R. Munter, Proc. Estonian Acad. Sci. Chem. 50 (2) (2001) 59–80.
[53] B. Kasprzyk-Hordern, Adv. Colloid Interface Sci. 110 (2004) 19–48.